



Journal Homepage: -[www.journalijar.com](http://www.journalijar.com)

## INTERNATIONAL JOURNAL OF ADVANCED RESEARCH (IJAR)

Article DOI:10.21474/IJAR01/10695  
DOI URL: <http://dx.doi.org/10.21474/IJAR01/10695>



### RESEARCH ARTICLE

#### DOPING DEPENDENCY ON ABSORPTION SPECTRUM OF INTRABAND TRANSITION BASED PHOTODETECTOR

Sumit Narayan Saurov

Department of Electrical and Electronic Engineering Ahsanullah University of Science and Technology 141 & 142, Love Road, Dhaka 1208, Bangladesh.

#### Manuscript Info

##### Manuscript History

Received: 20 January 2020

Final Accepted: 22 February 2020

Published: March 2020

##### Key words:-

Photodetector, Intersubband, Dipole Matrix Element, Absorption Coefficient, Photo-Excitation

#### Abstract

Intraband transition-based quantum cascaded photodetector is designed using GaN/AlN system. Carrier density distribution and dipole matrix element is calculated to determine the strength of optical transition. Doping effect on absorption spectrum has been investigated numerically.

Copy Right, IJAR, 2020,. All rights reserved.

#### Introduction:-

Photodetector is a special type of electrical device that converts optical signal directly into electrical signal. So, if light is given as an input to the photodetector than current or voltage is produced as an output. When radiating energy is absorbed by the electrons, they gain power and move into the upward energy levels. These excited charge carriers can be collected by placing electrodes across the device and then can be used to drive external loads. Photodetectors can play a vital role in renewable energy field as they can utilize solar energy or any other heat radiation. Day by day, demand of power is increasing beyond imagination. Fossil fuels are the major sources of power in present time. If this conventional energy source is exploited in this rate, there is a much higher probability of unavailability of this long-time dependable energy source in the next century. So, it is high time to take step of using renewable energy sources as a substitute of conventional energy sources. But even today, technology regarding the extraction of renewable energy is not developed so much. Only an insignificant percentage of available renewable energy sources is used to generate electricity. Special effort of developing technology regarding this field should be taken as early as possible to meet the challenge of increasing demand.

Photodetector can be classified in two groups. One of these is interband photodetector. In this detector, when light is absorbed by the valence band electrons, they move into conduction band. That means transfer occurs between two bands. As a result, free electron-hole pairs are created by photon absorption i.e., electron in the conduction band and hole in the valence band [1]. Another type of photodetector is intraband photodetector. Here, transition of electron occurs inside the same energy band. Holes have much higher effective mass than electrons. In case of a photodetector, faster carrier movement process is required to ensure larger current flow from the device. For this reason, only conduction band is important from design perspective [2]. Intraband i.e., intersubband transition-based photodetectors are normally designed to operate at infrared region of electromagnetic spectrum. Till date, different matured semiconductor systems are used to operate as an intersubband photodetector. Due to low conduction band offset, they operate at far-infrared or at best at mid-infrared region [3]. Systems having larger conduction band offset can be used to design detector which is capable of operating in near-infrared range. In present work, we are mainly concentrating on the group-III nitride based quantum cascaded photodetector heterostructure.

**Corresponding Author:- Sumit Narayan Saurov**

Address:- Department of Electrical and Electronic Engineering Ahsanullah University of Science and Technology 141 & 142, Love Road, Dhaka 1208, Bangladesh.

Doping is a very important parameter for intersubband photodetector in a view of design corner. Transition of electrons between different eigen energy levels depends on the available carrier density in those corresponding energy levels. Doping effect should be analyzed carefully to maximize absorption capability as well as to ensure faster relaxation process.

The organization of this paper is as follows: In Sec. II, we will present the design procedure of quantum cascaded heterostructure based photodetector. In Sec. III, we will analyze and calculate carrier density of different energy levels. In Sec. IV, we will investigate the doping dependency on the absorption capability numerically. In Sec. V, we will draw conclusions.

### Photodetector Heterostructure Design:

In this work, we have assumed that the GaN/AlN heterostructure is grown on Sapphire ( $\text{Al}_2\text{O}_3$ ) substrate. As GaN/AlN epitaxial layers are not fully lattice matched with Sapphire substrate, the designed structure is strain compensated. Though AlN and GaN can exist in the cubic zincblende phase, only the hexagonal wurtzite phase is thermodynamically stable. In the wurtzite phase, group-III nitrides form a continuous alloy system with direct bandgaps [4]. So, the total conduction band offset of the material system can be exploited for intersubband transitions. In this work, we have considered the wurtzite phase of nitrides. Here, GaN serves as a well material and AlN serves as a barrier material. These samples can be created by using either plasma assisted molecular beam epitaxy (PAMBE) or metal organic vapor phase epitaxy (MOVPE) process. The different parameter values that are important to design GaN/AlN heterostructures are given in Table I [4] – [8].

**Table I:-** Material Parameters of the System.

Parameters [unit]	GaN	AlN
Bandgap, $E_g$ [eV]	3.438	6.25
Effective mass, $m^*/m_0$	0.18	0.30
Refractive index, $n$	2.335	–
High Permittivity, $\epsilon_\infty$	5.31	4.35
Static Permittivity, $\epsilon_0$	10.2	9.32
LO-phonon energy, $\hbar\omega_{LO}$ [meV]	91.2	–

The valley conduction band diagram and the associated wavefunctions of designed quantum cascade structure have been shown in Fig. 1. We adjust the thickness of the barrier and well materials so that a broadband light absorption is possible. Here, we have doped in three quantum wells (QW). Optical transition will take place inside these three quantum wells. As a result, absorption of energy at different range is possible. To increase the current and hence the efficiency of the quantum cascade structures, as the carriers are photo-excited to the upper states, they should be available at the lower states of the next stage at a very short time. The fast transport of the excited carriers can be achieved by employing scattering due to Longitudinal Optical (LO) phonons. We design the structures so that the path through which the excited carriers relax is divided into steps of energy levels which differ in energy comparable to the LO phonon energy of the material system. The LO phonon energy of GaN material is 91.2 meV. In this structure, the energy spacing between any two consecutive levels in the relaxation path is between 80 to 110 meV. Therefore, carriers relax from the upper states of an active region to the lower states of the next active region at a faster rate.

We have designed the structure in such a way, that higher energy transition is possible for excited charge carriers. We have also ensured stronger transition after absorbing photons. Strength of an optical transition between two subbands depends on the dipole matrix element between them. Dipole matrix element does not depend on the doping. It depends on the electric dipole moment associated with the two states. In general, it is a complex vector quantity that includes the phase factors associated with the two states. Its direction gives the polarization of the transition, which determines how the system will interact with an electromagnetic wave of a given polarization. The dipole matrix element between two states  $i$ (initial) and  $f$  (final) is given by [9]

$$z_{ij} = \frac{\hbar}{2(E_j - E_i)} \langle \psi_j | p_z \frac{1}{m^*(E_j, z)} + \frac{1}{m^*(E_i, z)} p_z | \psi_i \rangle, \quad (1)$$

where  $m^*$  is the energy dependent effective mass and  $p_z$  is the momentum operator,  $E$  is the eigen energy level and  $\Psi$  is the probability function describing the availability of carrier at the corresponding state. Calculated dipole matrix element of different energy levels for these three doped wells of our designed structure has been shown in Table II.

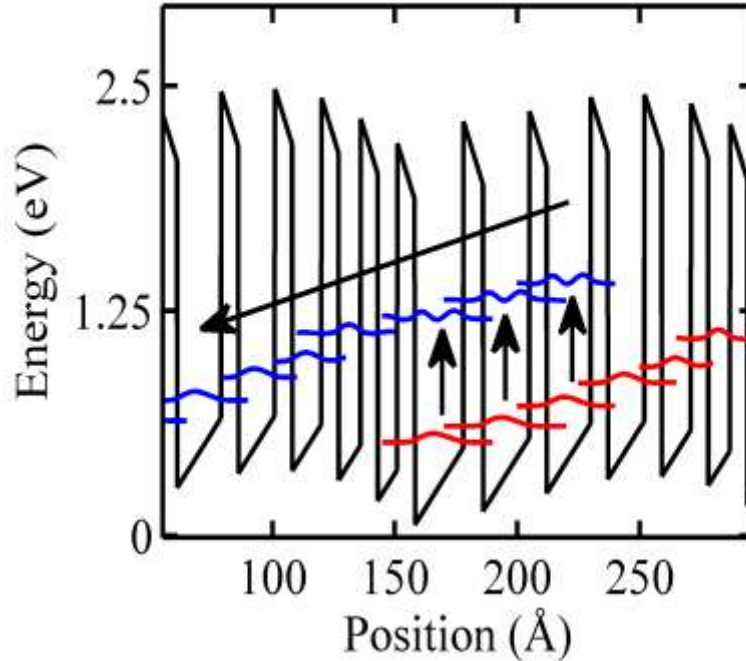


**Fig 1:-** Energy wavefunctions with squared envelope functions of the designed structure. The layer thicknesses (shown in Angstrom unit) of this designed structure are **7/20/7/19/7/18/7/15/7/12/7/9/7/8/7**. The numbers in bold fonts are AlN layers (barrier material) and the numbers in normal fonts are GaN (well material) layers. The underlined layer has been n-type doped. The photo-excitation of the carriers from one period (red coloured) to the next period (blue coloured) i.e., photon absorption process has been shown by the vertical arrow. The carrier relaxation from the upper energy levels to lower energy levels through subsequent stages i.e., photo-carrier collection process has been shown by the inclined arrow. The electric field  $F = 50$  kV/cm across the structure corresponds to the operating photovoltage point.

Higher value of dipole matrix element denotes the stronger interaction between subbands. So, stronger transition is possible between the lower energy levels and upper energy levels for our designed structure as dipole matrix elements are stronger for these corresponding energy levels. As a result, stronger absorption of optical illumination is possible.

**Table II:-** Dipole Matrix Element.

Doped QW	Initial Energy Level, i	Final Energy Level, f	Dipole Matrix element, $z_{ij}$ (Å)
1	3	22	1.2761
2	5	25	0.3628
3	8	29	0.3525

**Carrier Density Calculation:**

Number of available carriers in a definite energy state depends on the doping as well as density of states. In case of a quantum well, there are only two degrees of freedom. As a result, a two-dimensional electron gas is created inside the well. Density of states for a single subband in a quantum well can be calculated numerically using [10]

$$\rho^{2D}(E) = \sum_{i=1}^n \frac{m^*}{\pi \hbar^2} \Theta(E - E_i), \quad (2)$$

where,  $\Theta$  is the unit step function and  $n$  is total confined states within the quantum well system.

We have assumed that, before photo-excitation system is in thermal equilibrium. So, carriers are distributed among different energy levels according to Fermi-Dirac probability function as [10]

$$f(\varepsilon) = \frac{1}{e^{\frac{\varepsilon - E_F}{k_B T}} + 1}, \quad (3)$$

where  $k_B$  is the Boltzmann constant,  $T$  is the device temperature. As the photodetector operates in the room temperature,  $T$  is taken as 300 K. Here,  $E_F$  is the quasi-Fermi energy level which describes the carrier population within a subband. Quasi-Fermi distribution of carriers depends on the doping concentration. For a quantum well, we need to know the two-dimensional carrier density which is calculated by multiplying the doping density of the well by the thickness of the doped wells. If  $n_{2D}$  is the total carrier density than quasi-Fermi level,  $E_F$  can be calculated as [10]

$$n_{2D} = \frac{m^* k_B T}{\pi \hbar^2} \left\{ \left[ \frac{E_{\max} - E_F}{k_B T} - \ln \left( 1 + e^{\frac{E_{\max} - E_F}{k_B T}} \right) \right] - \left[ \frac{E_{\min} - E_F}{k_B T} - \ln \left( 1 + e^{\frac{E_{\min} - E_F}{k_B T}} \right) \right] \right\}, \quad (4)$$

where  $E_{\min}$  is the subband minima and  $E_{\max}$  is the top energy level of the quantum well.

Carrier density of energy levels where optical transition takes place plays a vital role to determine the absorption characteristics. As photon is absorbed by the electrons of the lower energy levels, there should be higher availability of electrons to utilize this optical power. After photon absorption, these electrons move to the upper energy level. So, there should be available empty states where photo-excited carriers will be moved. Lower carrier density at upper energy levels before photo-excitation is required to fulfill this requirement. As a result, stronger absorption directly depends on the carrier density difference between the two energy levels taking part in transition. At higher energy levels, there is less number of available carriers as carriers are mostly distributed in the lower energy levels. In our designed structure, absorption takes place in higher energy range. So, it can absorb electromagnetic radiation effectively and strongly. Two-dimensional carrier density of a state  $i$  with energy  $E_i$  can be calculated as [11]

$$N_i = \frac{m^* k_B T}{\pi \hbar^2} \ln \left( 1 + e^{\frac{E_F - E_i}{k_B T}} \right). \quad (5)$$

To calculate the effect of doping on carrier density distribution, we have considered two different doping. One is lower doping of  $N_{dop} = 10^{17}/m^3$  and other one is high doping with  $N_{dop} = 10^{26}/m^3$ . In present work, we will study and analyze the effect of these two different doping levels on the carrier density distribution as well as on absorption capability. Two-dimensional carrier density at different energy levels of three doped well in designed structure has been shown in Table III.

**Table III:-** Carrier Densities.

Eigen Energy Level	2D Carrier Density (no. / m <sup>2</sup> )	
	$N_{dop} = 10^{17}/m^3$	$N_{dop} = 10^{26}/m^3$
3	$4.60 \times 10^8$	$2.89 \times 10^{17}$
5	$2.48 \times 10^7$	$2.32 \times 10^{17}$
8	$4.26 \times 10^5$	$1.52 \times 10^{17}$
22	0	$1.15 \times 10^{10}$
25	0	$2.69 \times 10^8$
29	0	$6.68 \times 10^5$

So, by higher doping, larger carrier density difference between the energy levels can be achieved. But excess heavy doping can cause random tunneling through barrier. Different secondary leakage mechanisms will be significant resulting in uncertain behavior of photo-detection process. Moreover, excess carrier density requires greater time to relax to lower energy levels resulting slower carrier relaxation process. As a result, higher power generation process will be interrupted. So, for effective design moderate doping should be taken. Normally group-III nitride based quantum well heterostructure is doped at a range of  $1 \times 10^{23}/m^3$  to  $1 \times 10^{26}/m^3$  [4].

### Absorption Spectrum:

Absorption coefficient ( $\alpha$ ) is the measurement of how well a device absorbs energy from the optical source. Higher value of this coefficient denotes higher absorption ability of the structure. In our work, we have considered two-dimensional absorption coefficient ( $\alpha_{2D}$ ) that means absorption coefficient is normalized to the stage inverse thickness. The absorption spectrum can be calculated using [12]

$$\alpha_{2D}(\hbar\omega) = \sum_{i \in gl} \sum_{j \in el} \frac{q^2 z_{ij}^2 \omega}{nc\epsilon_0} (N_i - N_j) \cdot \frac{\Gamma_{ij} / 2}{(E_j - E_i - \hbar\omega)^2 + (\Gamma_{ij} / 2)^2}, \quad (1)$$

where “gl” denotes the ground energy levels and “el” denotes the upper excited energy levels. The ground energy levels are at the bottom of vertical arrow and the upper excited energy levels are on the top of the vertical arrows in Fig. 1. Here,  $\omega$  is the radian frequency,  $n$  is the refractive index,  $c$  is the velocity of the light,  $q$  is the charge of an electron,  $\epsilon_0$  is the static dielectric constant of quantum well material,  $z_{ij}$  is the dipole matrix element,  $E_j$  is the energy value of upper level and  $E_i$  is the energy value of lower level. The line width of absorption spectrum,  $\Gamma_{ij}$ , has been assumed to be 11% of the transition energy  $E_j - E_i$ [4].

So, absorption coefficient is directly proportional to the carrier density difference,  $N_i - N_j$  as shown in Eq. (6). Stronger absorption coefficient along with wider bandwidth denotes the capability of absorbing electromagnetic optical radiation effectively by the photodetector structure. These requirements can be obtained by creating carrier density difference between the corresponding energy levels i.e., by changing doping level.

Absorption coefficient is plotted against absorbed photon energy for  $N_{dop} = 10^{26}/m^3$  in Fig. 2. There are two major peaks in the absorption spectrum. They are at 596 meV and 704 meV. Peak absorption coefficient is almost  $3 \times 10^{-5}$  which is at 704 meV. So, our designed structure can absorb from almost 550 meV to 850 meV of available solar energy as shown in Fig. 2. Linewidth i.e., bandwidth of absorption spectrum is considered as Full-Width at Half-Maximum (FWHM). Effective bandwidth is almost 180 meV for this doping level.

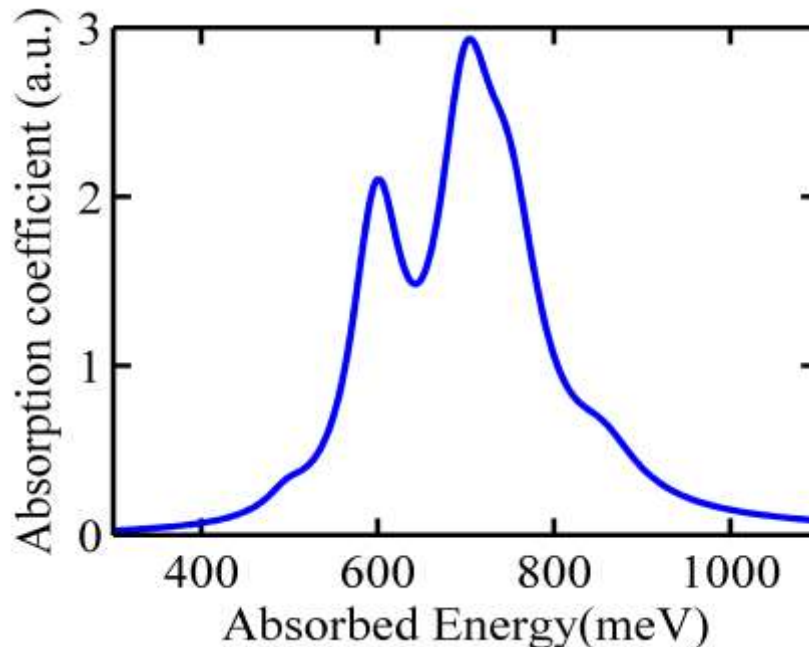


**Fig 2:-** Absorption spectrum for  $N_{dop} = 10^{26}/m^3$ . Absorption coefficient is normalized with respect to  $1 \times 10^{-5}$ .

Absorption coefficient is plotted against absorbed photon energy for  $N_{dop} = 10^{17}/m^3$  in Fig. 3. Absorption peaks are in the same energy level. It does not depend on the doping concentration as peak absorption coefficient occurs at the energy difference of two levels where transition takes place as shown in Eq. (6). But peak absorption coefficient is almost  $2.5 \times 10^{-15}$  for this low doped structure. So, absorption capability decreases in a large scale. To absorb

photons, enough electrons should be available at lower energy levels. Otherwise, only a small portion of available photon energy will be used. In case of low doping, there are very few charge carriers available in ground states. So, energy transferred by these charge carriers is also small. Linewidth for this doping is only about 90 meV. So, bandwidth also decreases for low doping. As bandwidth is a measurement of effective absorbed energy range, lower doping results in ineffective design of photodetector. Absorbed optical power leads to the generation of photocurrent which is used to drive external loads. So, narrow bandwidth of a structure denotes lower generation of current. As a result, less power will be generated from this designed structure. So, low doping leads to lower efficiency quantum well photodetector. So, doping should be increased at a certain higher level to absorb more electro-magnetic radiation as well as to avoid secondary leakage effects.

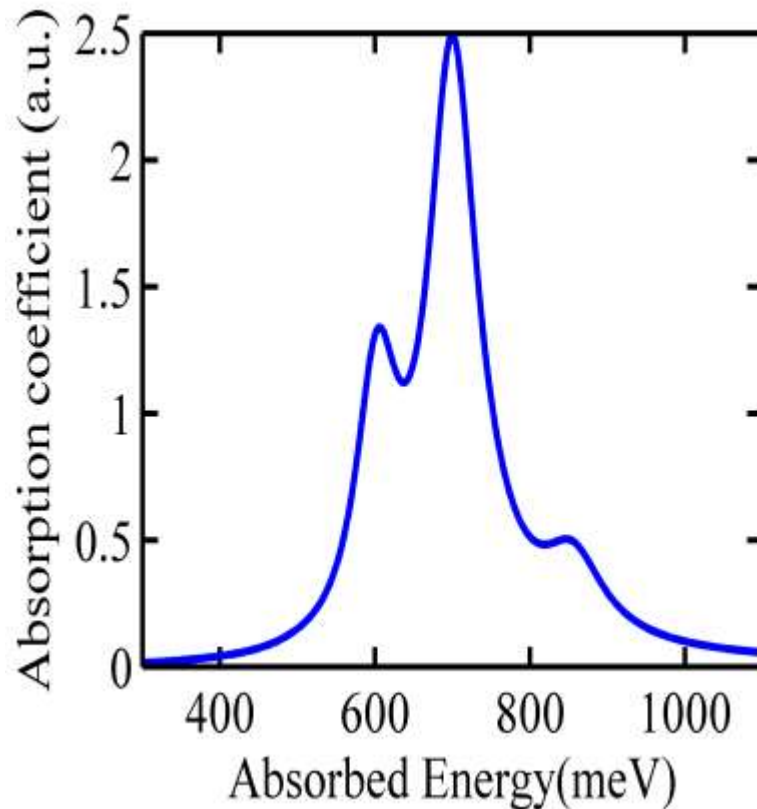


Fig 3:- Absorption spectrum for  $N_{dop} = 10^{17}/m^3$ . Absorption coefficient is normalized with respect to  $1 \times 10^{-15}$ .

### Conclusions:-

In summary, we have shown that, absorption spectrum of a quantum well cascaded heterostructure is strongly dependent on the doping density. Higher doping leads to stronger absorption coefficient and wider bandwidth in comparison to lower doping. As excess heavy doping leads to the rise of different non-linear secondary effects and random tunneling probability, moderate doping should be introduced to design an effective photodetector.

### Acknowledgment:-

The author would like to acknowledge the support from the department of Electrical and Electronic Engineering (EEE) of Ahsanullah University of Science and Technology (AUST) in carrying out this work.

### References:-

1. S. O. Kasap, Optoelectronics and Photonics: Principles and Practices, New Delhi: Pearson Education Inc., 2009.
2. S. M. Sze and K. K. Ng, Physics of Semiconductor Devices, 3rd ed., New Jersey: John Wiley & Sons Inc., 2007.
2. R. Paiella, Intersubband Transitions in Quantum Structures, New York: McGraw-Hill, 2006.

3. E. Baumann, "Near infrared intersubband absorption and photovoltaic detection in GaN/AlN multi quantum well structures," Ph.D. dissertation, Department of Physics, University of Neuchâtel, Neuchâtel, Switzerland, Sep. 2007.
4. M. E. Levinshtein, S. L. Rumyantsev, and M. S. Shur, Properties of advanced semiconductor materials: GaN, AlN, InN, BN, SiC, SiGe, New York: John Wiley and Sons, 2001.
5. I. Vurgaftman and J. R. Meyer, "Band parameters for nitrogen-containing semiconductors," J. Appl. Phys., vol. 94, pp. 3675-3696, Jun. 2003.
6. W. J. Moore, J. A. Freitas, R. T. Holm, O. Kovalenkov, and V. Dmitriev, "Infrared dielectric function of wurtzite Aluminum Nitride," Appl. Phys. Lett., vol. 86, pp. 141912-1—141912-3, Apr. 2005.
7. T. Azuhata, T. Sota, K. Suzuki, and S. Nakamura, "Polarized Raman-spectra in GaN," J.Phys.: Condens. Matter, vol. 7, pp. 129-133, Mar. 1995.
8. H. C. Liu and F. Capasso, Intersubband Transitions in Quantum Wells: Semiconductors and Semimetals, San Diego: Academic Press, 2000.
9. P. Harrison, Quantum Wells, Wires and Dots: Theoretical and Computational Physics , Chichester: John Wiley and Sons, 1999.
10. D. Jena, "Bandstructure in Low-Dimensional Structures," Department of Electrical Engineering, University of Notre Dame, 2004.
11. M. Helm, Intersubband transitions in quantum wells: physics and device applications I, San Diego: Academic Press, 2000.